



Research paper

Cordierite from a high-temperature low-pressure shear zone of the south-western Bohemian Massif (Moldanubian terrain, Austria)



Robert Sturm

Brunnleitenweg 41, A-5061 Eibseehen, Austria

ARTICLE INFO

Article history:

Received 23 March 2016

Received in revised form 27 October 2016

Accepted 28 October 2016

Editorial handling - Dr. J. Jacek Puziewicz

Keywords:

Shear zone

Cordierite

Mylonite

Geothermobarometry

Bohemian Massif

ABSTRACT

A medium-scale shear zone exposed in the gneiss rocks of the South-western Bohemian Massif (Moldanubian Zone) contains cordierite, whose Na p.f.u. is subject to a significant increase from the centre to the edge of the deformation area, whilst other elements only show negligible variations. Coexisting mineral phases of cordierite include garnet, biotite, and sillimanite. According to the results obtained from the garnet-cordierite $\text{Fe}^{2+}/\text{Mg}^{2+}$ -exchange thermometer a decrease of peak temperature from 639 °C in the central mylonite to 593 °C in the marginal mylonite can be observed, which indicates significant shear heating. Lithological pressures were estimated by considering the position of cordierite-forming reactions in the P-T field and the stability of coexisting sillimanite. They are subject to a reduction from 0.35 GPa in the highest deformed mylonite to 0.31 GPa at the margin of the shear zone. According to the results of comprehensive petrographic and mineralogical studies the investigated shear zone underwent a Variscan HT-LP metamorphic event implying the formation of cordierite and an Alpine MT-LP event entailing the rotation and decomposition of the cordierite phase.

© 2016 Elsevier GmbH. All rights reserved.

1. Introduction

Ductile shear zones are planes of finite displacement between two lithological blocks and form, when the hardening capacity of the host material has been exceeded (e.g. [White et al., 1980](#); [Steyer and Sturm, 2002](#); [Sturm and Steyer, 2003](#)). Due to their rather limited sizes, ranging from few centimeters to meters, ductile shear zones offer excellent possibilities to study the metamorphic evolution of the wall rock as well as chemical and mechanical changes within a predefined transect of increasing deformation. Where shear zones cut pelitic to semipelitic rocks, calculations of metamorphic pressures and temperatures can be easily realized due to numerous mineral reactions during the shearing event. P-T estimations have been carried out for lots of shear zones in the Alps and the Bohemian Massif (e.g. [Selverstone et al., 1991](#) and references therein; [Wallbrecher et al., 1993](#)). In the ductile shear zone of the present study, the mineral cordierite has formed during prograde and peak metamorphism and therefore will stand in the midpoint of the following investigations.

Cordierite is a (Mg, Fe)Al-silicate which is characterized by a wide range of natural occurrences. As outlined in numerous publications (see review in [Deer et al., 1992](#); [Bertoldi et al., 2004](#)), cordierite mainly crystallizes in thermally metamorphosed rocks,

particularly those derived from argillaceous sediments. Additionally, the mineral can be a major constituent of parageneses formed under high-grade regional metamorphism. [Harker \(1939\)](#) found that the metamorphic formation of cordierite is generally restricted to conditions of deficient or low shearing stress producing only moderate pressures. With rising pressure due to transpression cordierite often breaks down to enstatite and sillimanite or, at higher temperature, to sapphirine and quartz ([Seifert, 1976](#); [Spear, 1993](#)). Besides its crystallization in metamorphic rocks, cordierite is also found in specific igneous rocks like peraluminous granites and related high-grade anatexic terrains ([Clarke, 1995](#); [Barbey et al., 1999](#)). Here, the mineral is considered as a product of subsolidus metamorphic reactions ([Pereira and Bea, 1994](#)), a product of peritectic reactions at the granite source ([Wall et al., 1987](#); [Groppo et al., 2013](#)) or a derivative of argillaceous material contaminating the granitic magma. Among some authors cordierite is also considered as a cotectic magmatic mineral (e.g. [Clarke, 1981](#); [Clemens and Wall, 1981](#); [Groppo et al., 2013](#)) or a mineral phase formed by metasomatism, which directly followed the process of granitization ([Didier and Dupraz, 1985](#)). Cordierite of gem quality frequently occurs in granite pegmatites, where it usually crystallizes from uncontaminated pegmatitic liquids. A previous crystallization from residual magmas enriched with Al-silicates is also discussed.

This study presents a detailed analysis of the mylonites exposed in a shear zone and, as the main feature, an extensive description of the cordierite blasts formed during the shearing event. The contribution pursues three main objectives: First, the shear zone

E-mail address: sturm.rob@hotmail.com

described here offers the possibility of studying cordierite formation within a short-range transect of several tens of meters; second, shear-related crystallization of cordierite and its geothermobarometric evaluation have not been documented very frequently in the past and are therefore in the focus of this study; and third, due to the fact that shear zone rocks have passed two metamorphic events, besides cordierite formation also decomposition of this mineral phase is visualized.

2. Geological setting of the study area

The studied rocks as well as their surrounding lithology can be assigned to the south-western margin of the Bohemian Massif. This Variscan orogen is mainly located within the Central-European Moldanubian Zone (Kossmat, 1927; Fig. 1a), characterized by widespread high-temperature low-pressure metamorphism, partial melting processes and extensive plutonism. As outlined by numerous authors (e.g. Matte, 1986; Franke, 1989, 2000), the central part of the Bohemian Massif mainly consists of the Moldanubian unit which includes the Teplá-Barrandium primarily acting as a micro-continent (Fig. 1b). The Moldanubian unit can be subdivided into the high-temperature high-pressure Gföhl unit (Medaris et al., 1995, 1998, 2005, 2006; Schulmann et al., 2005, 2008; Štípká et al., 2008), the Ostrong unit (Monotonous Series) containing high-temperature low-pressure migmatites and gneisses, and the Drosendorf unit, a gneiss complex with marbles, calc-silicates, and amphibolites (Varied series; Zoubek, 1965; O'Brien and Vrána, 1995; O'Brien, 1997; Petrakakis, 1986, 1997; Schulmann et al., 2008).

The geology of the study area is characterized by Variscan migmatites and gneisses of the Monotonous series that were intruded by post-Variscan granite bodies (Frasl and Finger, 1991 and references cited therein; Fig. 1c). Another essential feature of the regional geology are the tertiary, NW-SE tending strike-slip faults (Pfahl and Danube fault) with variable shear sense, which divided the lithology into three main granitic bodies (Fuchs and Thiele, 1968; Fuchs and Matura, 1976; Wallbrecher et al., 1993; Fig. 1c). The rocks of the present study were formed in a local dextral shear zone that can be interpreted as a side branch of the Pfahl fault which itself runs from the Bavarian forest to the Rodl valley (Fig. 1c). The quarry, in which the cordierite-bearing mylonites are accessible, is located near the village Unterurasch, around 50 km northwest of Linz. It consists of two orthogonal walls, which are between 60 and 80 m long and up to 30 m high (Fig. 2). On the WSW-ENE-tending wall mylonites with increasing grades of deformation are exposed. The centre of the shear zone is indicated by a fine-grained, blue- to grey-coloured ultramylonite with only few clasts of K-feldspar relics (Fig. 3a, b). When approaching the shear zone walls, the number and size of these clasts increases continuously. The protolith of the shear zone could not be found in the quarry itself, but was sampled about 100 m away from the centre of deformation (Fig. 1c). This educt rock determined by chemical analyses and comparative zircon studies (Sturm, 2004) represents a remarkably layered granitoid that mainly consists of K-feldspar, plagioclase and biotite (Fig. 3a). As outlined by Sturm (1995, 2004, 2010), the respective granitoid can be recognized as a specific variety of the so-called Pearl Gneiss which is one of the main granitoid bodies in the study area (see above).

3. Rock sampling and analytical methods

Samples of the cordierite-bearing rocks were collected in the quarry described above. Besides the highest deformed mylonite in the center of the shear zone also rocks showing lower grades of deformation were sampled along a defined transect (Fig. 2b).

The protolith of the shear zone was sampled about 100 m outside the center of deformation. All investigated rocks are quite homogeneous as concerning the grain size, and therefore sample size was generally limited to ca. 10 kg, respectively. Part of the samples was used for the production of oriented thin sections, and part was crushed for the separation of cordierite and accessory minerals. From each sample at least one polished thin section was produced for microchemical analysis. This was carried out on a JEOL JXA-8600 microprobe at the Institute of Geology, University of Salzburg. Operating parameters were 30 nA beam current, 15 kV accelerating voltage, 10 s counting time for each element except Ti and Na (30 s), and a constant beam diameter of 1 μm. Natural and synthetic silicates and oxides served as standards for the main element analysis. Correction of the raw analyses was conducted by the application of an internal ZAF-4 procedure. The produced element analyses were affected by an average error not exceeding 0.1 wt.%. For Na₂O the detection limit was 0.050 wt.% employing operating parameters as detailed above. Backscattered electron imaging (BSEI) of altered cordierites was carried out by using a beam current that ranged from 30 nA to 40 nA in order to increase the contrast for photography.

Calculation of peak temperatures within the shear zone was mainly conducted by application of the garnet-cordierite Mg/Fe²⁺-exchange thermometer published by Perchuk and Lavrent'eva (1983). Estimation of a minimum pressure was realized using the cordierite stability field and the cordierite-involving reactions as published in conventional petrogenetic grid (Spear, 1993). In addition, pressures could be determined by using the original P-T diagram of Holdaway and Lee (1977) as well as the related refinements recently published by Dachs and Geiger (2008).

Modal compositions of the studied rocks were estimated by using an eyepiece with counting grid and applying appropriate stereological methods (determination of the total number of points hitting the mineral phases of interest, respectively). In order to obtain highly accurate modal amounts for each mineral phase occurring in a specific rock, thin sections with variable orientations (N = 3) were subjected to the counting procedure. For estimation of the clast/matrix ratio in mylonites with different grades of deformation, it was clarified first that [1] clasts include all mineral grains exceeding a diameter of 5 mm and [2] K-feldspar, plagioclase, and cordierite (formed during the late-Variscan HT-LP metamorphic event) represent the main mineral phases producing such large grains. Relative volumes of clasts and matrix minerals contained in the sample rocks were again found by stereological techniques. The quantity-based relationship between quartz relics and recrystallized quartz grains was determined in a similar fashion. Differentiation between relic grains and recrystallized grains was conducted with the help of characteristic recrystallization textures occurring in the mylonite samples and extensive grain size analyses.

4. Petrography and mineral chemistry of the analyzed rocks

The cordierite-bearing mylonites are grey- to blue-coloured rocks characterized by a weak stretching lineation. The metamorphic schistosity is evident in the oriented thin sections. The mylonites uniformly display assemblages containing the mineral phases K-feldspar + quartz + plagioclase + cordierite + biotite + white mica + sillimanite (fibrolite) + garnet + chlorite + ilmenite (Table 1). Under the microscope the investigated samples show a matrix formed by very fine-grained quartz and biotite. Both minerals are recrystallized in high amounts (Fig. 5b, 6a-d) and can be concentrated to specific domains or layers. Biotite is often associated

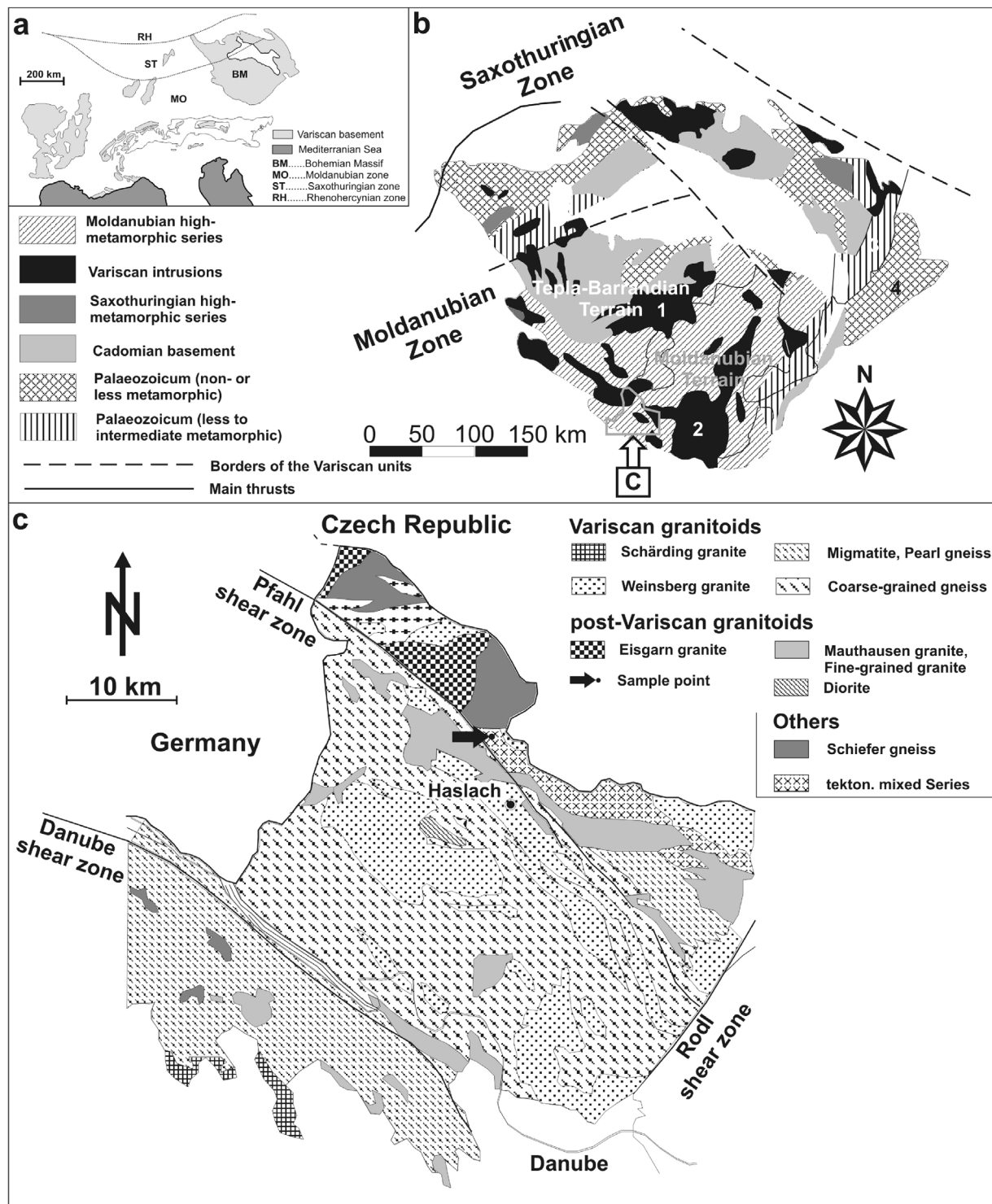


Fig. 1. a) Map of the Variscan basement located in Central Europe with its main geological units, b) Simplified geological map of the Bohemian Massif with coarse tectonometamorphic subdivision (1 · Central-Bohemian pluton, 2 · Bohemian pluton, 3 · Moravo-Silesicum, 4 · Sudeticum), c) Geological map of south-western margin of the Bohemian Massif with the most important lithological units exposed there and the position of the shear zone investigated in this study (Fuchs and Matura, 1976).

with fibrolitic sillimanite and muscovite. The porphyroclasts and –blasts of the rock are mainly represented by feldspar relics and cordierite and partly show a significant rotation parallel to the deformation plane. As documented in Fig. 4b, the clast-matrix ratio is affected by remarkable changes from the edge to the centre of the shear zone, ranging from 0.63 to 0.20. While isometric clasts have been often excluded from Alpine deformation, anisometric clasts

are marked by phenomena like kinking, undulatory extinction, or the generation of polysynthetic pressure twins (plagioclase). Large grains of K-feldspar are sometimes affected by the formation of core-mantle textures, thereby expressing high temperatures during Variscan deformation. In the pressure shadow of larger crystals fine grains of recrystallized quartz, biotite, or an opaque phase (e.g. ilmenite) are accumulated. Cordierite is often surrounded

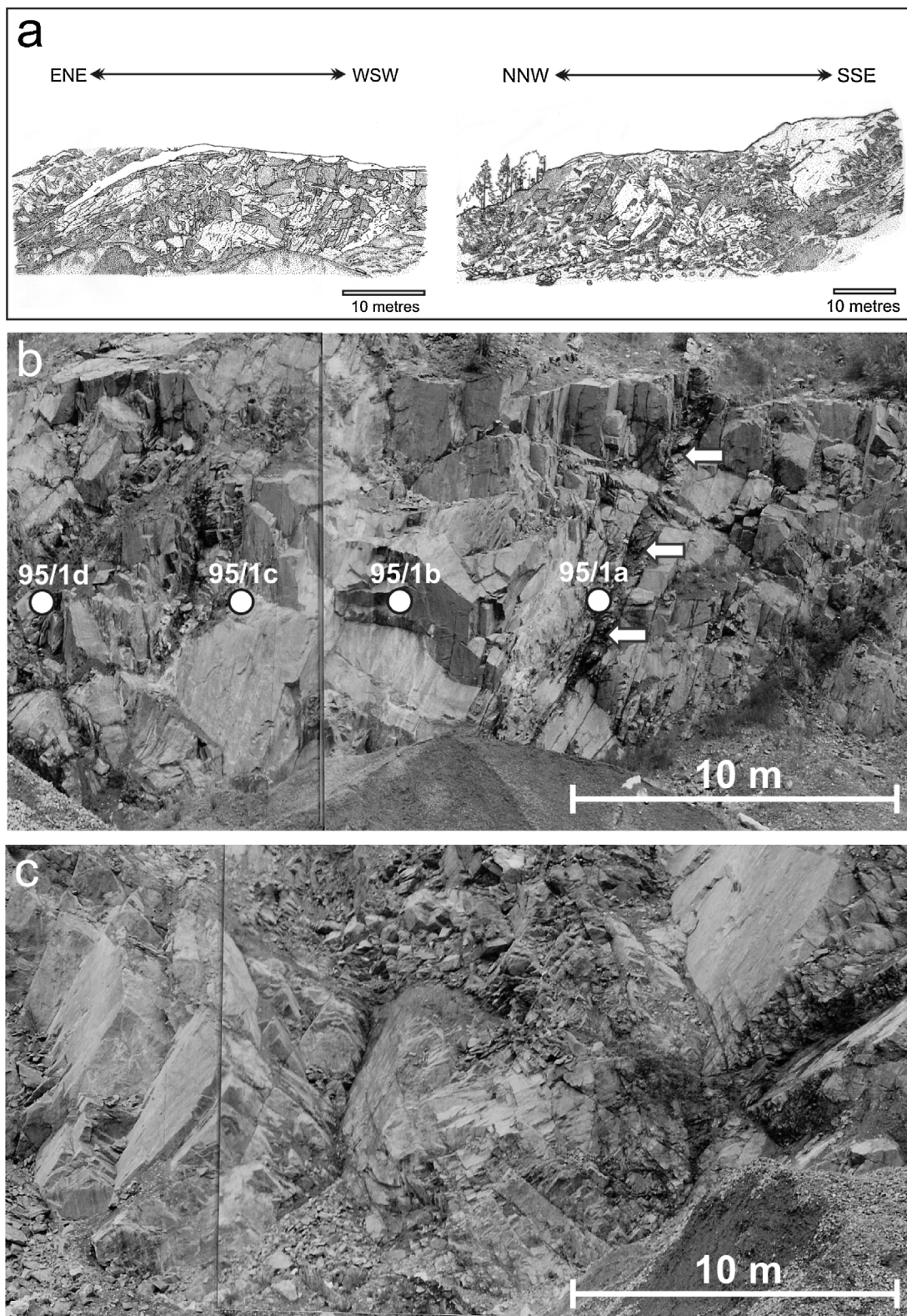


Fig. 2. a) Illustration of the quarry, within which the central part of the shear zone is exposed; b) Detail photography of the ENE-WSW tending wall of the quarry with the position of the single mylonite samples; c) Photography of the NNW-SSE tending wall of the quarry. The protolithic rock was collected about 100 m east of the quarry.

by muscovite and biotite which are the products of retrograde decomposition reactions. In the mylonitic rocks different stages of cordierite pinitization can be observed (see below). The main accessory minerals of the cordierite-mylonite are zircon, mon-

azite, apatite, and xenotime. As outlined in the graph of Fig. 4a, the modal composition of the mylonite is characterized by only slight changes throughout the shear zone, but differs significantly from that of the Perl Gneiss representing the protolith of deformation.

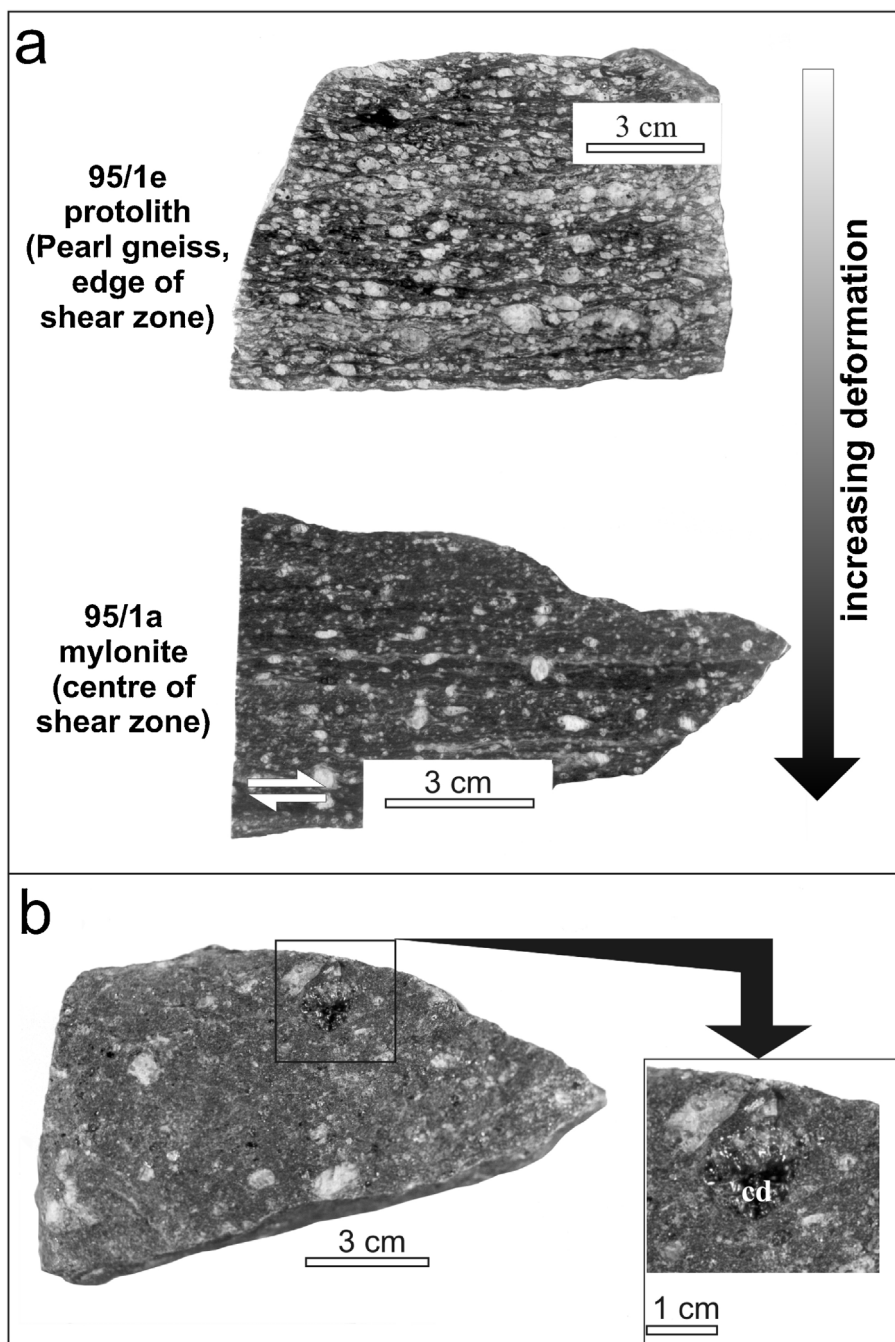


Fig. 3. Selection of rocks sampled in- and outside the quarry introduced in Fig. 2: a) Protolith of the shear zone (Pearl Gneiss) exhibiting an evidently layered texture with single oligoclase crystals being arranged like in a pearl chain (sample 95/1e) and mylonite in the centre of the shear zone (sample 95/1a) with its fine-grained matrix and fewer feldspar clasts, b) Sample of the mylonite including a large cordierite crystal with dark-blue colour.

This is mainly expressed by a remarkable decrease of plagioclase and increase of quartz. Sillimanite, garnet, and cordierite are not observed in the wall rock of the shear zone.

In Table 1 representative analyses of the main constituents (except cordierite) of the cordierite mylonites are listed. Mylonitic K-feldspar is characterized by orthoclase contents between 91 and 95%, while the concentration of the albite component varies between 4.5 and 8%. Anorthite content does never exceed 1.0%. Plagioclase shows a chemical composition, which is mainly dominated by albite (73–76%). All analyzed grains also contain remarkable amounts of orthoclase, ranging from 1.0 to 2.5%. Biotite shows a slight predominance of the annite component with the Fe/(Fe + Mg) ratio ranging from 0.505 to 0.530. The concentration of TiO₂ varies

between 0.80 and 1.20 wt.%, whereas the content of MnO does not exceed 1.0 wt.%. Tetrahedral Al ranges from 1.16 to 1.30 atoms per formula unit and therefore deviates significantly from the ideal value of 1.00. White mica shows great fluctuations concerning its chemical composition. While the analysis listed in Table 1 is marked by a muscovite content of ca. 90%, other crystals can contain rather high amounts of phengite. The detection of Ti in mica indicates a secondary formation out of biotite. Phengite-rich crystals can be interpreted as products of cordierite decomposition. The mineral garnet is dominated by almandine ranging from 73 to 74%. The content of spessartine varies between 12 and 15%, whereas pyrope content fluctuates around 10% and grossular content around 2%.

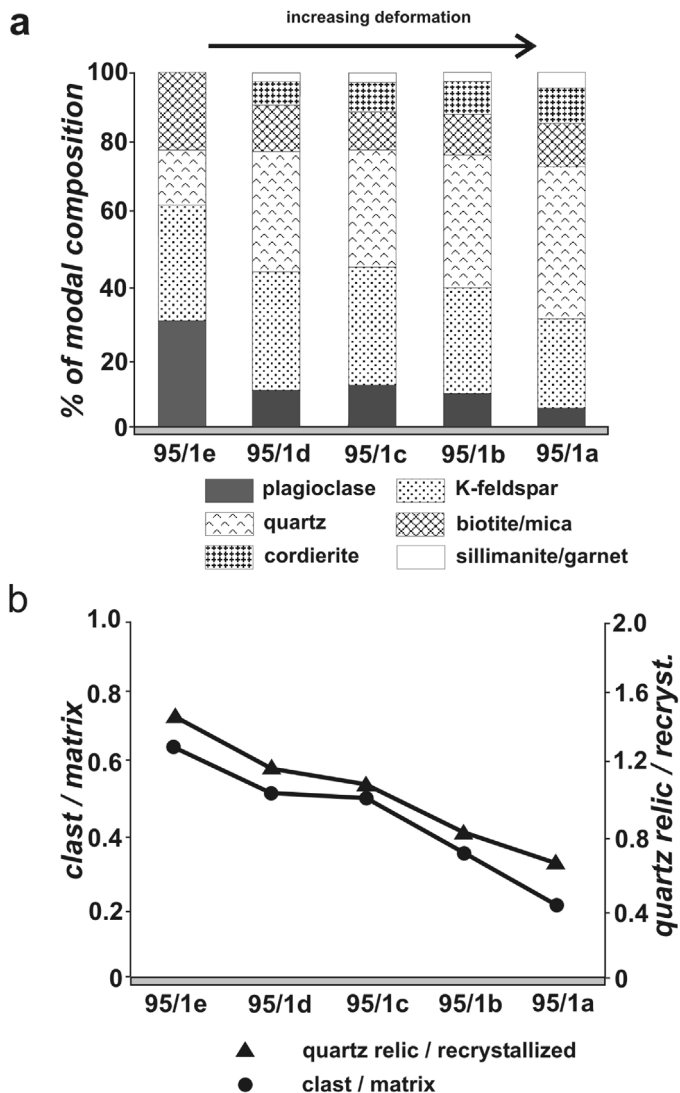


Fig. 4. a) Modal composition of shear zone rocks exhibiting different grades of deformation, b) Ratio between relic quartz and recrystallized quartz (triangle) and clast-matrix ratio (circle) and their dependence on the grade of rock deformation.

5. Results of the cordierite studies

5.1. Macroscopic and microscopic appearance of cordierite

The mylonites of the ductile shear zone contain cordierite crystals ranging from 0.3 to 10 mm in size. Large cordierites which are not or only slightly affected by pinitization are characterized by a medium- to dark-blue colour (Fig. 3b). With progressing decomposition of the mineral, its colour changes continuously to bluish-green. Although cordierite has been subjected to shear-induced rotation and partly extensive decomposition, there exists clear evidence for the crystallization of this mineral phase during the earlier HT-LP metamorphic event. As demonstrated in Fig. 4a, modal composition of protolithic and mylonitic rocks is marked by a continuous increase of the amount of cordierite from the margin to the centre of the shear zone (note: the protolith being located outside the quarry does not contain cordierite at all). Besides this increase in volume also a permanent size increase of the cordierite grains from least to most highly deformed mylonites can be observed, representing a strong indicator for cordierite growth during Variscan deformation.

Under the optical microscope cordierites appear as isometric to slightly elongated grains surrounded by a fine-grained matrix of quartz, biotite, white mica, and sillimanite. Those grains not affected by pinitization are well identifiable due to dark cracks and coronas as well as their typical pleochroism. While ca. 30% of the grains are free from inclusion phases, ca. 70% contain quartz, primary biotite, sillimanite, and garnet (Fig. 5a, b). Like feldspar most crystals are only slightly rotated parallel to the displacement plane, indicating mainly transpressional (oblate) deformation with only small influence of simple shear. The mylonites offer the possibility of studying various stages of cordierite decomposition, ranging from only poorly affected grains to fully transformed pinites (Fig. 6a-d). In a first stage, cracks running through the mineral are continuously filled with very fine crystals of mica and chlorite (Fig. 6a). Subsequently, the margins of cordierite are transformed into muscovite, sillimanite and biotite of variable size (Fig. 6b). In a medium stage of decomposition, internal pinitization undergoes a significant progression, forming aggregates of mainly mica, biotite, and chlorite (Fig. 6c). In the last stage of pinitization, the former cordierite has been fully transformed into bluish-green pinite which is demarcated from the matrix by a mantle of muscovite and biotite crystals. If the decomposition process is accompanied by local shear strain, the resulting pinite blast is marked by sigmoid shape and internal micro-crenulations (Fig. 6d).

When studied with the electron microprobe in the backscattered-electron mode, pinites show a fine discontinuous corona of replacing minerals which itself is surrounded by large grains of biotite and muscovite (Fig. 6e). This outer corona demarcates the blast from the surrounding matrix as well as adjacent feldspar clasts and relic quartz.

The genetic relationship between the minerals biotite, sillimanite, and muscovite may be regarded as rather complex. According to microscopic studies of the mylonitic matrix, biotite and sillimanite developed specific intergrowth textures which indicate equilibrium of both mineral phases during cordierite formation. Here it has to be stated clearly that biotite associated with sillimanite does not exhibit significant chemical differences with respect to that occurring as regular matrix mineral or inclusion in large crystals. Muscovite, on the other hand, has to be interpreted as late mineral phase occurring as recently as cordierite starts to decompose. This later fact is mainly underlined microscopically by the preferential occurrence of fine muscovite crystals within and around cordierite grains that underwent pinitization.

5.2. Major-element composition of the mylonitic cordierite

Microprobe analyses of cordierite crystals from the mylonitic rocks of the shear zone show that the mineral is characterized by a rather homogeneous chemistry (Table 2). In contrast to the ideal structural formula of cordierite, a slight deficiency in Si (<5.0 p.f.u.) and excess in Al (>4.0 p.f.u.) can be observed. The sum of both tetrahedral cations varies between 9.030 and 9.080 and therefore deviates from the ideal value of 9.00 by 0.3–0.8%. The replacement of octahedral Mg by Fe²⁺ and Mn is documented by a Mg/(Mg + Fe²⁺ + Mn) ratio ranging from 0.543 to 0.584. These values confirm a predominance of Mg in the octahedral sites. MnO plays a minor role in the major-element composition, reaching a maximum value of 0.74 wt.% (Table 2). The sum of all octahedral cations ranges from 1.900 to 1.965, deviating from the ideal formula by 2–5%. CaO and K₂O could be sometimes detected in very low amounts (0.002–0.009 wt.% and 0.001–0.002 wt.%, respectively) and therefore seem to be of negligible importance concerning the occupation of the crystal channels. In contrast, Na₂O is represented in the channels with a concentration varying between 0.42 and 0.57 wt.%. This alkali metal is, together with Al, mostly responsible for the cation excess above 11.00. The sum of alkali metals and Ca in the struc-

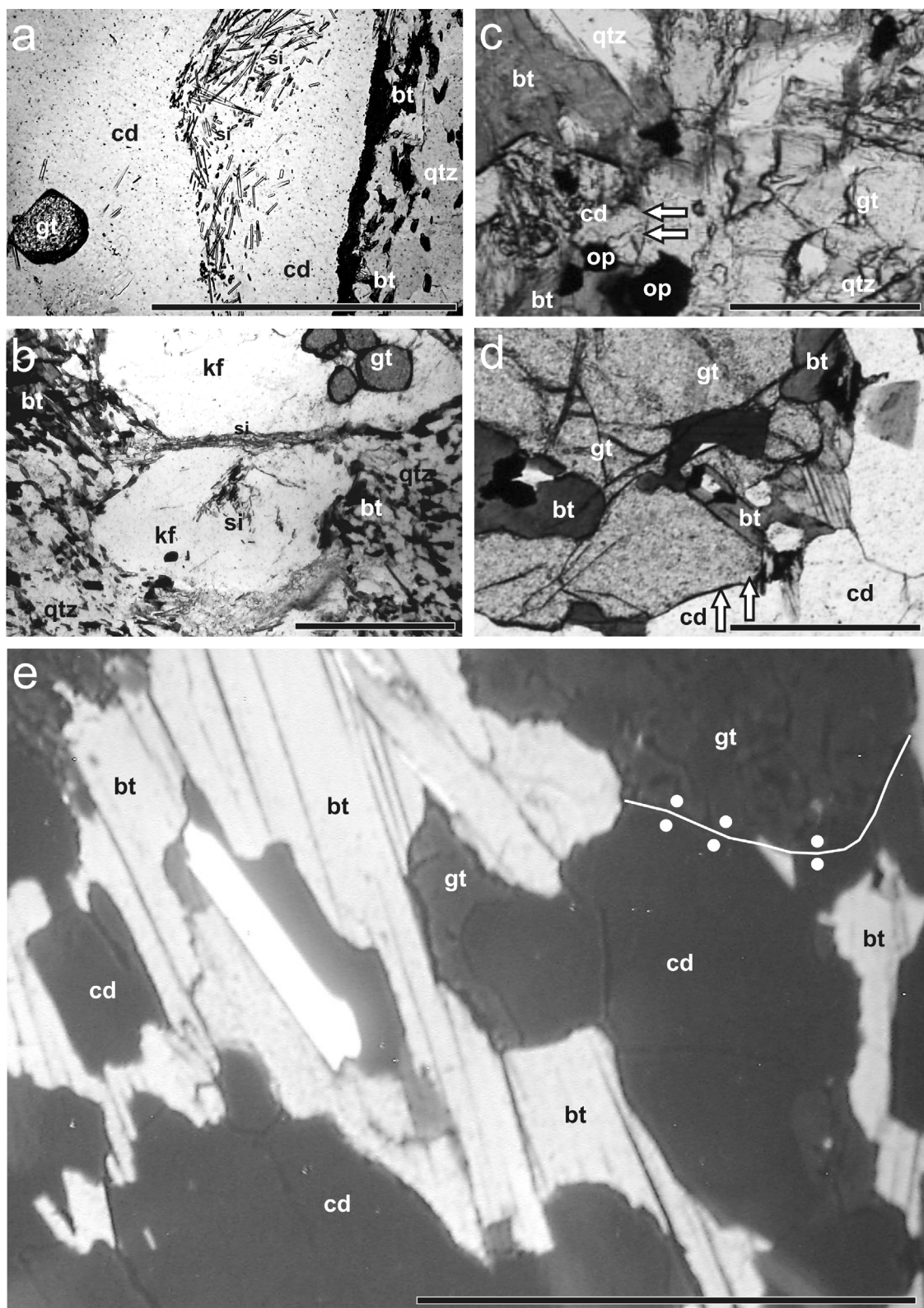


Fig. 5. Micrographs with mineral assemblages partly visualizing the cordierite-forming reactions [1] and [2] documented in the text: a) inclusions of garnet and sillimanite in cordierite; b) inclusions of garnet and sillimanite in K-feldspar; c) and d) coexistence of cordierite and garnet (arrows); e) backscattered electron image of coexisting garnet and cordierite with analysis points for $\text{Fe}^{2+}/\text{Mg}^{2+}$ -exchange thermometry (bars: 1 mm). Abbreviations: bt...biotite, cd...cordierite, gt...garnet, kf...K-feldspar, ms...muscovite, op...opaque phase, plg...plagioclase, qtz...quartz, si...sillimanite.

tural formula ranges from 0.089 to 0.120 (Table 2). The formulae listed in Table 2 yield evidence that the insertion of Na and K into the channels is mainly caused by a coupled substitution of (Na, K)

+ Al against channel site + Si. The sum of all analyzed oxides ranges from 97.07 wt.% to 98.16 wt.% suggesting the introduction of about 2 wt.% of volatile compounds (H_2O , CO_2) into the crystal lattice.

Table 1

Representative microprobe analyses of the main minerals (except cordierite) from the mylonites of the investigated shear zone.

| Sample | 95/01a | | | | | | 95/01b | | | 95/01c | | | 95/01d | | | |
|--------------------------------|--------|--------|-------|--------|-------|-------|--------|--------|--------|--------|--------|--------|--------|--------|--------|-------|
| | kf | plg | bt | ms | gt | gt | kf | plg | bt | gt | plg | bt | gt | plg | bt | gt |
| SiO ₂ | 64.51 | 62.92 | 35.57 | 46.33 | 37.18 | 37.15 | 65.23 | 62.94 | 35.66 | 36.99 | 62.64 | 36.12 | 37.23 | 61.96 | 36.05 | 36.95 |
| TiO ₂ | --- | --- | 1.19 | 0.3 | --- | --- | --- | --- | 1.11 | --- | --- | 0.75 | --- | --- | 0.89 | --- |
| Al ₂ O ₃ | 18.68 | 23.42 | 20.31 | 36.7 | 20.75 | 18.35 | 23.27 | 20.26 | 22.56 | 23.32 | 20.56 | 20.73 | 23.85 | 20.23 | 20.87 | |
| FeO | --- | --- | 18.18 | 0.95 | 32.49 | 31.98 | --- | --- | 18.33 | 32.17 | --- | 18.76 | 31.98 | --- | 19.23 | 32.15 |
| MgO | --- | --- | 9.48 | 0.61 | 2.63 | 2.57 | --- | --- | 9.62 | 2.54 | --- | 9.26 | 2.65 | --- | 8.76 | 2.65 |
| MnO | --- | --- | 0.67 | --- | 5.84 | 6.12 | --- | --- | 0.73 | 6.5 | --- | 0.78 | 5.87 | --- | 0.84 | 6.05 |
| CaO | 0.05 | 5.03 | --- | --- | 0.76 | 0.89 | 0.02 | 4.95 | --- | 0.8 | 4.98 | --- | 0.84 | 5.42 | --- | 0.75 |
| K ₂ O | 15.6 | 0.43 | 9.97 | 9.52 | --- | --- | 15.16 | 0.43 | 9.73 | --- | 0.62 | 9.98 | --- | 0.42 | 10.25 | --- |
| Na ₂ O | 0.7 | 8.52 | 0.12 | 0.48 | --- | --- | 0.87 | 8.52 | 0.08 | --- | 8.62 | 0.16 | --- | 8.43 | 0.04 | --- |
| Total | 99.54 | 100.26 | 95.49 | 94.89 | 99.66 | 99.46 | 99.63 | 100.11 | 95.54 | 99.56 | 100.18 | 96.37 | 99.3 | 100.08 | 96.29 | 99.42 |
| ΣO | 16 | 16 | 22.22 | 16 | 16 | 16 | 16 | 22 | 16 | 16 | 22 | 16 | 16 | 22 | 16 | 16 |
| Si | 5.98 | 5.55 | 5.47 | 6.134 | 3.016 | 3.018 | 6.02 | 5.56 | 5.42 | 3.012 | 5.55 | 5.428 | 3.025 | 5.497 | 5.446 | 3.005 |
| Ti | --- | --- | 0.18 | 0.037 | --- | --- | --- | --- | 0.16 | --- | --- | 0.085 | --- | --- | 0.101 | --- |
| Al ^{IV} | 2.04 | 2.44 | 2.53 | 1.866 | --- | --- | 1.99 | 2.42 | 2.58 | --- | 2.453 | 2.572 | --- | 2.513 | 2.554 | --- |
| Al ^{VII} | --- | --- | 1.33 | 3.846 | 2 | 2.002 | --- | --- | 1.06 | 1.988 | --- | 1.097 | 2.001 | --- | 1.075 | 2.015 |
| Fe | --- | --- | 2.33 | 0.105 | 2.205 | 2.173 | --- | --- | 2.33 | 2.191 | --- | 2.358 | 2.173 | --- | 2.429 | 2.187 |
| Mg | --- | --- | 2.16 | 0.11 | 0.319 | 0.311 | --- | --- | 2.18 | 0.308 | --- | 2.075 | 0.321 | --- | 1.973 | 0.321 |
| Mn | --- | --- | 0.08 | --- | 0.402 | 0.421 | --- | --- | 0.009 | 0.448 | --- | 0.099 | 0.404 | --- | 0.107 | 0.417 |
| Ca | 0.006 | 0.48 | --- | --- | 0.066 | 0.077 | 0.001 | 0.47 | --- | 0.07 | 0.473 | --- | 0.073 | 0.515 | --- | 0.065 |
| K | 1.849 | 0.04 | 1.95 | 1.607 | --- | --- | 1.784 | 0.05 | 1.88 | --- | 0.07 | 1.913 | --- | 0.048 | 1.975 | --- |
| Na | 0.123 | 1.48 | 0.04 | 0.124 | --- | --- | 0.17 | 1.49 | 0.002 | --- | 1.481 | 0.047 | --- | 1.45 | 0.012 | --- |
| Total | 9.998 | 9.99 | 16.07 | 13.838 | 8.006 | 8.003 | 9.945 | 9.99 | 15.621 | 8.017 | 10.027 | 15.674 | 7.997 | 10.024 | 15.673 | 8.01 |

Table 2

Representative microprobe analyses of cordierites from the mylonite of the investigated shear zone. Stoichiometric calculations were carried out on the basis of 18 oxygen anions including Na, K, and Ca.

| Sample No. | 95/01a | | | 95/01b | | | 95/01c | | 95/01d | |
|--------------------------------|--------|--------|--------|--------|--------|--------|--------|--------|--------|--------|
| | 1 | 2 | 3 | 4 | 5 | 6 | 7 | 8 | 9 | 10 |
| SiO ₂ | 47.58 | 47.86 | 47.9 | 48.06 | 47.77 | 48.05 | 47.84 | 47.83 | 47.96 | 47.51 |
| Al ₂ O ₃ | 32.69 | 32.54 | 32.55 | 32.76 | 32.67 | 32.66 | 32.94 | 32.71 | 32.52 | 32.86 |
| FeO | 8.85 | 8.99 | 8.89 | 9.31 | 9.17 | 9.41 | 9.54 | 9.86 | 9.68 | 9.22 |
| MgO | 6.75 | 7.13 | 7.33 | 6.92 | 6.96 | 7.05 | 6.78 | 6.45 | 6.82 | 6.55 |
| MnO | 0.74 | 0.55 | 0.41 | 0.39 | 0.41 | 0.4 | 0.52 | 0.48 | 0.45 | 0.62 |
| CaO | 0.03 | 0.03 | --- | 0.09 | 0.03 | --- | 0.02 | 0.03 | 0.05 | 0.04 |
| K ₂ O | 0.01 | 0.01 | --- | 0.02 | --- | --- | --- | --- | --- | --- |
| Na ₂ O | 0.42 | 0.47 | 0.45 | 0.51 | 0.49 | 0.5 | 0.52 | 0.53 | 0.57 | 0.54 |
| Total | 97.07 | 97.58 | 97.53 | 98.07 | 97.5 | 98.07 | 98.16 | 97.89 | 98.05 | 97.34 |
| Si | 4.994 | 4.998 | 4.998 | 4.998 | 4.993 | 4.998 | 4.979 | 4.997 | 5 | 4.981 |
| Al ^{T1} | 1.006 | 1.002 | 1.002 | 1.002 | 1.007 | 1.002 | 1.021 | 1.003 | 1 | 1.019 |
| Al ^{T2} | 3.069 | 3.034 | 3.032 | 3.044 | 3.049 | 3.032 | 3.049 | 3.055 | 3.026 | 3.073 |
| Fe | 0.777 | 0.785 | 0.776 | 0.81 | 0.802 | 0.819 | 0.83 | 0.861 | 0.844 | 0.808 |
| Mg | 1.056 | 1.11 | 1.14 | 1.073 | 1.085 | 1.093 | 1.052 | 1.005 | 1.066 | 1.024 |
| Mn | 0.066 | 0.049 | 0.037 | 0.034 | 0.036 | 0.036 | 0.046 | 0.042 | 0.04 | 0.055 |
| Ca | 0.003 | 0.003 | --- | 0.011 | 0.004 | --- | 0.002 | 0.003 | 0.006 | 0.004 |
| K | 0.001 | 0.001 | --- | 0.003 | --- | --- | --- | --- | --- | --- |
| Na | 0.085 | 0.095 | 0.091 | 0.103 | 0.099 | 0.101 | 0.105 | 0.108 | 0.114 | 0.109 |
| Total | 11.058 | 11.078 | 11.076 | 11.014 | 11.074 | 11.081 | 11.085 | 11.074 | 11.09 | 11.073 |

As could be established by several analyses on a single grain, cordierite from the mylonites does not show significant compositional zoning due to a possible variation of the Mg/(Mg + Fe²⁺ + Mn) ratio from the crystal core to its rim. The respective ratio fluctuates between 0.561 and 0.566 (Table 2, analyses 5 and 6), but does not follow any remarkable trend. It must be noted that many cordierites of this microchemical investigation are characterized by a marginal replacement by pinite, which could be a reason for the destruction of a former compositional zoning.

6. Estimation of temperatures and pressures during deformation

Temperatures of mylonitization were estimated using the garnet-cordierite Fe²⁺/Mg²⁺-exchange thermometer of Perchuk and Lavrent'eva (1983), which is based on a wide set of experimental data and includes the effect of Ca and Mn in garnet on the calculated temperature. Garnet-cordierite temperatures were

computed with the mean values for X_{Mg}(grt) and X_{Mg}(crd) listed in Table 3. Within a presumed pressure interval of 0.30–0.40 GPa, mean temperatures range from 593 to 639 °C. Due to interrelationships between several included variables a uniform error of ±15 °C was assumed (Fig. 7a, b).

Estimation of pressures is mainly based on assumptions concerning the formation of cordierite and related mineral reactions, the stability of cordierite and its dependence on the Mg/(Mg + Fe) ratio, and the stability of other mineral constituents. A very coarse evaluation of pressure during metamorphism is possible by the fact that fibrolithic sillimanite is the only AlSiO₅ phase occurring in the studied mylonites. Considering a temperature range of 570–630 °C and the stability field of sillimanite within the system kyanite-andalusite-sillimanite (Holdaway, 1971; Hemingway et al., 1991), pressure had to be higher than ca. 0.30 GPa.

As mentioned in the chapter dealing with cordierite petrography, numerous cordierite grains are marked by inclusions of quartz, biotite, sillimanite, and garnet. Except for sillimanite, all included

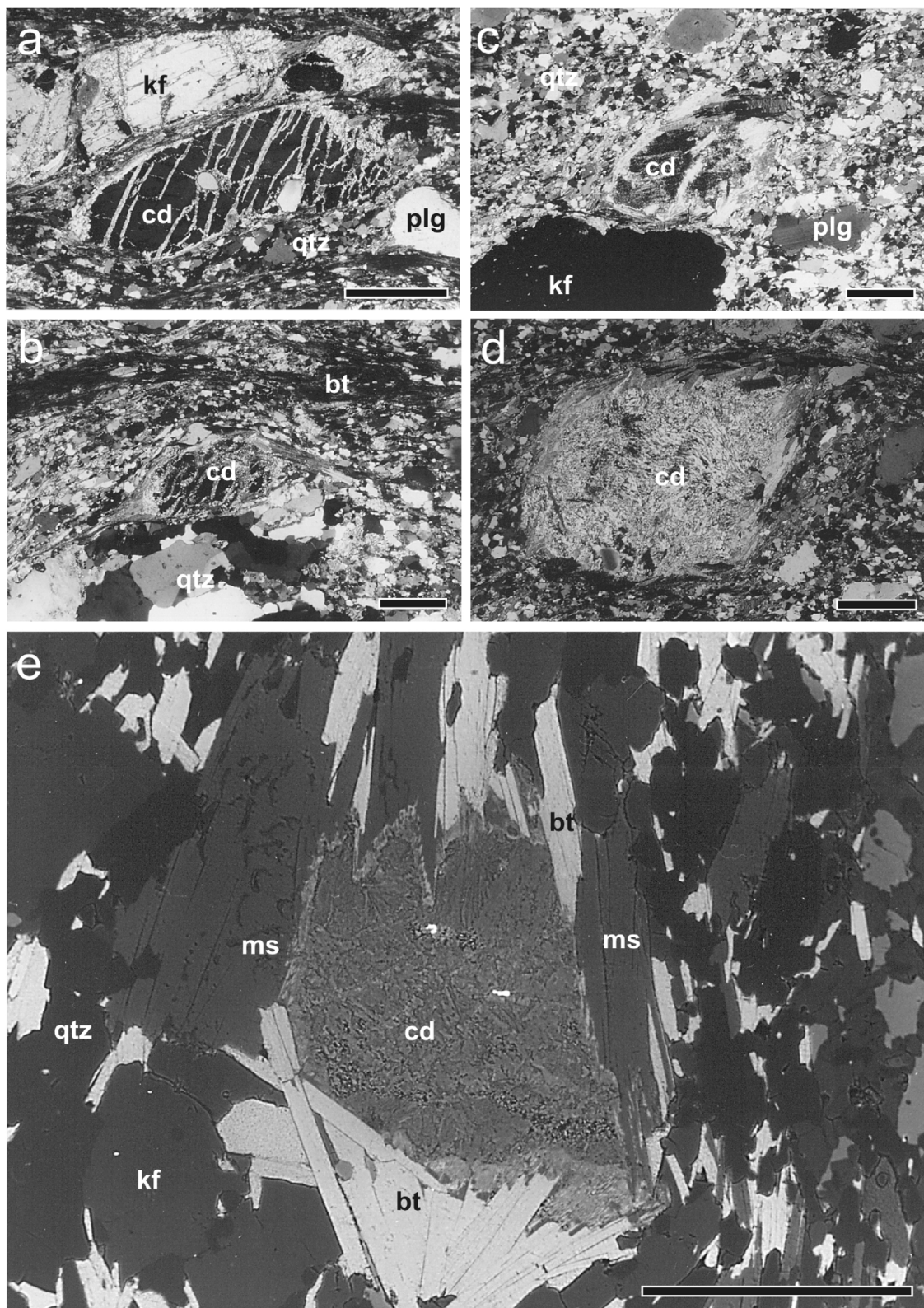


Fig. 6. Microscopic occurrence of cordierite in the rocks of the investigated shear zone: a-d) micrographs showing different grades of cordierite decomposition that took place during retrograde metamorphism (see text; bars: 1 mm); e) backscattered electron image of cordierite and surrounding mineral phases (bar: 1 mm). Abbreviations: see Fig. 5.

minerals are also constituents of the wall rock and therefore have crystallized before the shearing event. Since muscovite plays a minor role in the wall rock and chlorite is not contained at all, for-

mation of metamorphic cordierite may be considered according to the following reactions:

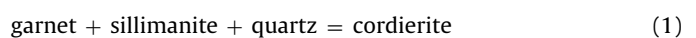


Table 3

Table 3
Important mineral parameters and related temperatures.

| Sample | X _{Mg} (crd) | X _{Mg} (grt) Na(crd) | | T _{PL} [°C] |
|--------|-----------------------|-------------------------------|---------------|----------------------|
| | m ± stdev | m ± stdev | m ± stdev | |
| 95/01a | 0.565 ± 0.012 | 0.127 ± 0.008 | 0.092 ± 0.006 | 639 |
| 95/01b | 0.556 ± 0.015 | 0.113 ± 0.006 | 0.101 ± 0.007 | 618 |
| 95/01c | 0.552 ± 0.016 | 0.106 ± 0.009 | 0.105 ± 0.004 | 604 |
| 95/01d | 0.545 ± 0.014 | 0.099 ± 0.005 | 0.110 ± 0.005 | 593 |

Abbr.: T_{PL} ...temperature according to the garnet-cordierite Fe/Mg exchange thermometer of Perchuk and Lavrent'eva (1983).

$X_{Mg} = Mg / (Mg + Fe^{2+} + Mn)$; $Na(crd) = Na$ p.f.u. in cordierite.

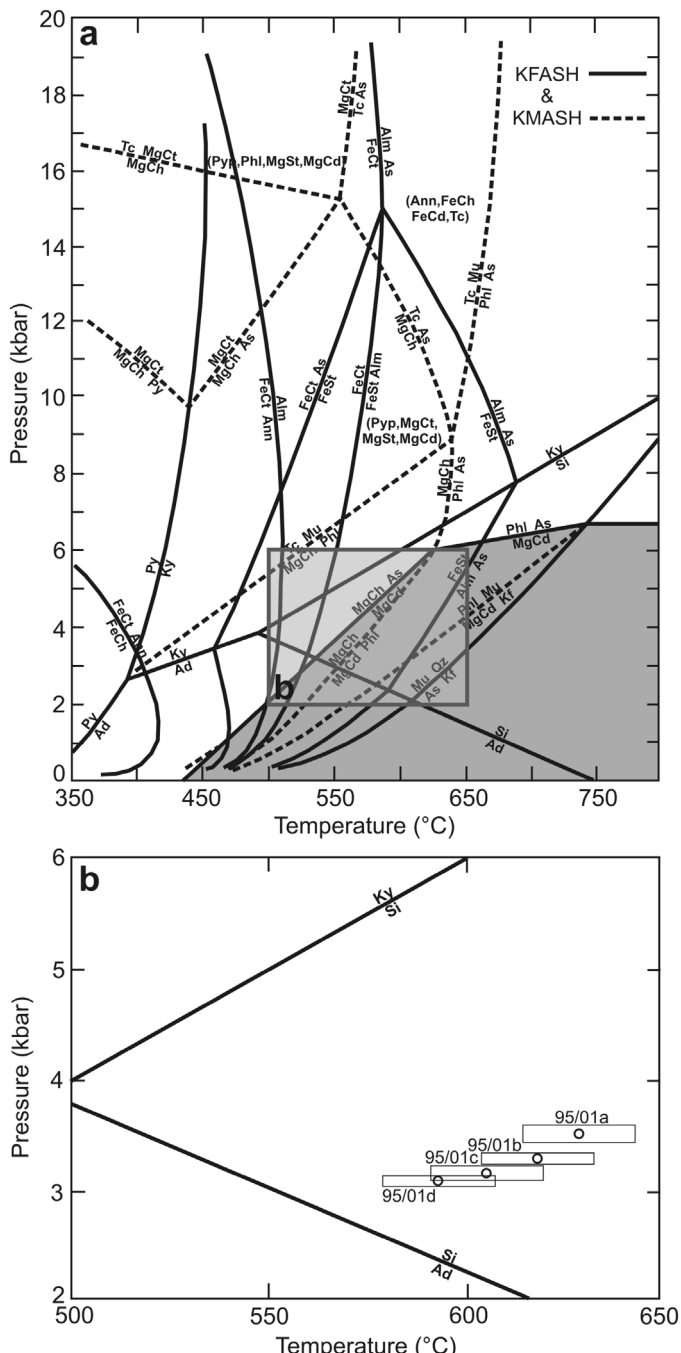


Fig. 7. a) P-T diagram illustrating important reaction isogrades of the KFASH and KMASH system (Spear, 1993) as well as the stability field of cordierite (grey-shaded); b) Detailed P-T diagram with plotted samples of the cordierite shear zone

$$\text{biotite} + \text{sillimanite} + \text{quartz} = \text{cordierite} + \text{garnet}$$



Both reactions are typical for high-Si gneisses affected by regional or mechanic metamorphism. While Reaction (1) mainly occurs during amphibolite-facies metamorphism, Reaction (2) has to be assigned to granulite-facies events. Holdaway and Lee (1977) have investigated both reactions experimentally for various $Mg/(Mg + Fe)$ ratios of cordierite. Plotting the calculated temperatures into the graph provided by the authors and determining the respective composition of cordierite results in pressures between 0.31 and 0.35 GPa during cordierite formation. Similar to temperature also pressure decreases continuously from the centre to the edge of the shear zone. According to these estimations, formation of the investigated shear zone can be classified as a high-temperature low-pressure event (Fig. 7b).

An important question concerns the microstructural relationships between garnet and cordierite which are essential for purposeful application of geothermometry. Since formation of cordierite was primarily performed according to Reaction (2) noted above, garnet was mostly consumed during HT-LP mylonitization, but may be observed as inclusion phase in cordierite in isolated cases (Fig. 5a, c). Also fibrolitic sillimanite represents an occasionally occurring inclusion phase in preserved cordierite crystals (Fig. 5a). In this case no thermodynamically defined equilibrium between cordierite and garnet or between cordierite and sillimanite may be attested. In some zones exempted from maximum strain small coexisting grains of cordierite and garnet may be found which enable application of Mg^{2+}/Fe^{2+} -exchange thermometry (Fig. 5c–e).

During the uplift of the mylonitic rocks, metamorphic cordierite was affected by two main breakdown reactions. Both of them can be easily recognized under the microscope. The breakdown of cordierite to coexisting biotite and sillimanite (Reaction (2)) can be testified by fine coronas of these minerals around old grains of cordierite. Biotite and sillimanite are oriented parallel to the displacement plane. As another reaction which has been described in detail above, cordierite is decomposed to muscovite, and chlorite according to the following equilibrium:



As outlined by [Yardley \(1990\)](#), this process of pinitization starts at temperatures between 475 °C and 500 °C and can continue, until hydrothermal P-T conditions are reached. Since some cordierite grains are fully substituted by very fine pinite, Reaction (3) has played a major role during the uplift of the mylonitic rocks during the Alpine tectonometamorphic event.

7. Discussion

As outlined in the present study, cordierite may occur as a major constituent in high-temperature low-pressure mylonites which have developed from high-Al granitoids. Many publications of the past have shown that cordierite mainly crystallizes during events of contact metamorphism and high-grade regional metamorphism (e.g. Deer et al., 1992; Schreyer et al., 1990; Kalt et al., 1998). Also a magmatic crystallization and natural occurrence in pegmatites have been described by numerous authors (e.g. Clarke, 1981, 1995; Clemens and Wall, 1981; Didier and Dupraz, 1985; Wall et al., 1987; Barbey et al., 1999; Groppe et al., 2013). As demonstrated by Groppe et al. (2013) for the exemplary case of cordierite-bearing anatetic rocks of the higher Himalayan crystallines in eastern Nepal, extensive microstructural analyses in association with melt production and/or melt consumption allow a differentiation between peritectic and cotectic cordierite. Both types of cordierite are produced under LP conditions, which corresponds to the results of the present study, and at temperatures ranging from 670 to 700 °C.

Formation of the mineral during a shearing process was believed to be only possible at deficient or low shearing stress (Harker, 1939). This is mainly due to the sensitiveness of cordierite to high pressures, causing a breakdown to enstatite or sapphirine + quartz (Seifert, 1976; Spear, 1993). Whilst for anhydrous cordierite breakdown reactions take place at about 0.6 GPa, for hydrous cordierite the respective reaction isogrades are generally shifted to lower pressures. Based on extensive temperature and pressure calculations, for the shear zone of this study maximal P-T conditions of 630 ± 15 °C and 0.35 GPa could be estimated. This indicates a mylonitization at a high- to medium-crustal level and corresponds very well with the stability data of hydrous cordierite.

Increase of temperature from the margin to the centre of the shear zone (Fig. 7b) may be interpreted as the result of extensive shear heating. In the past this phenomenon was regarded to contribute significantly to crustal events characterized by prograde metamorphism. Theoretical computations of this process, on the other side, could demonstrate that it is unlikely to be of prime importance (Leloup et al., 1999). However, a similar increase of temperature was also documented for the Karlstift shear zone, representing a NNE-SSW tending strike-slip fault which is about 60 km away from the sample location (Brandmayr et al., 1999).

Fe-Mg exchange equilibria used as geothermometers (garnet-biotite, garnet-cordierite) are affected by several drawbacks such as their sensitiveness to retrograde diffusion (Elphick et al., 1985; Spear, 1991), chemical zoning of garnet or the transformation of biotite to chlorite during a retrograde overprint of the host rock. All these phenomena may significantly hamper the calculation of peak temperatures due to changes of the Fe-Mg ratios. Alternatively, Kalt et al. (1998) tested the reliability of the Na-in-cordierite thermometer (Mirwald, 1986) by its application to contact-metamorphic rocks exposed on the island of Kos. Temperatures derived from this thermometer were consistent with constraints from experiments and petrogenetic grids. They were also very similar to those temperatures derived from respective Fe-Mg equilibria. The authors concluded that mainly in the temperature range of 508–762 °C the Na-in-cordierite thermometer represents a very useful tool as long as a_{Na} is buffered at a minimum level by sodic plagioclase. As a further conclusion, the Fe content of cordierite does not remarkably affect the calculated temperatures. However, due to a lack of more current data supporting this conclusion, the thermometer was not used in the present study. The behaviour of Na-in-cordierite, on the other side, corresponds with the results outlined by Kalt et al. (1998) and increases the necessity of further studies on this topic.

As outlined in detail by Büttner (1999), shearing under enhanced thermal conditions along the Pfahl shear zone has been documented for few exposures hitherto (e.g. Masch and Cetin, 1991). The

author further states that in many strike-slip zones this high-grade event has been partially overprinted by later amphibolite-facies and greenschist-facies deformation. In correspondence with the shear zone presented in this contribution, high temperature is chiefly indicated by a synkinematic growth of cordierite and sillimanite within the other exposures, whereby both minerals are aligned parallel to the mylonitic structures. According to Büttner (1999) both the Schlieren granite and the Weinsberg granite (both free of cordierite) are commonly assumed as protoliths for the cordierite-sillimanite-mylonites, whereas the (cordierite-containing) Pearl gneisses are not believed to act as educts of local deformation. This is mainly justified by the circumstance that cordierite in Pfahl mylonites differs from that in the Pearl gneisses in size, abundance, and chemical composition. The Pearl gneiss variety of the study presented here is either completely free of cordierite (Fig. 4a) or contains a few volume-percent of this mineral phase. As demonstrated by Sturm (1995, 2004, 2010), the granitoid can be undoubtedly related to the cordierite-sillimanite-mylonite of this contribution after comparison of the zircon populations included in the respective rocks.

Concerning the pressure conditions during the shearing process estimated for the mylonite of this contribution, an excellent agreement with the results presented by Büttner (1999) may be recognized. By using the geobarometer outlined by Holdaway and Lee (1977) and the related improvements presented by Dachs and Geiger (2008) the author calculated a pressure of 3.3–4.0 kbar (0.33–0.4 GPa), being effective at the high-T stage of the Pfahl shear zone. According to current results from geological and petrologic studies the high-T shearing event resulting in the cordierite-sillimanite-mylonite was preceded by solidification processes of locally intruded magmas, which took place at temperatures of 700 ± 30 °C and pressures of 3.8–5.0 kbar (0.38–0.5 GPa). After mylonite formation most high-T rocks exposed along the Pfahl shear zone were subject to a greenschist-facies overprint, leading e.g. to the partial decomposition of cordierite blasts.

From the results of this study it can be concluded that cordierite can be a major mineral constituent of a high-temperature low-pressure shear zone and can be also used as a potential tool for the calculation of peak temperatures during the metamorphic event.

References

- Štípká, P., Schulmann, K., Powell, R., 2008. Contrasting metamorphic histories of lenses of high-pressure rocks and host migmatites with a flat orogenic fabric (Bohemian Massif, Czech Republic): a result of tectonic mixing within horizontal crustal flow? *J. Metamorph. Geol.* 26, 623–646.
- Büttner, S.H., 1999. The geometric evolution of structures in granite during continuous deformation from magmatic to solid-state conditions: an example from the central European Variscan Belt. *Am. Mineral.* 84, 1781–1792.
- Barbey, P., Margnac, C., Montel, J.M., Macaudière, J., Gasquet, D., Jablon, J., 1999. Cordierite growth textures and the conditions of genesis and emplacement of crustal granitic magmas: the Velay granite complex (Massif Central, France). *J. Petrol.* 40, 1425–1441.
- Bertoldi, C., Proyer, A., Garbe-Schönberg, D., Behrens, H., Dachs, E., 2004. Comprehensive chemical analyses of natural cordierites: implications for exchange mechanisms. *Lithos* 78, 389–409.
- Brandmayr, M., Loizenbauer, J., Wallbrecher, E., 1999. Contrasting P-T conditions during conjugate shear zone development in the Southern Bohemian Massif, Austria. *Mitt. Österr. Geol. Ges.* 90, 11–29.
- Clarke, D.B., 1981. The mineralogy of peraluminous granites: a review. *Can. Miner.* 19, 3–17.
- Clarke, D.B., 1995. Cordierite in felsic igneous rocks: a synthesis. *Min. Mag.* 59, 311–325.
- Clemens, J.D., Wall, V.J., 1981. Crystallization and origin of some peraluminous (S-type) granites. *Can. Miner.* 19, 111–131.
- Dachs, E., Geiger, C.A., 2008. Low-temperature heat capacity of synthetic Fe- and Mg-cordierite: thermodynamic properties and phase relations in the system $FeO-Al_2O_3-SiO_2-(H_2O)$. *Eur. J. Mineral.* 20, 47–62.
- Deer, W.A., Howie, R.A., Zussman, J., 1992. *An Introduction to the Rock-Forming Minerals*. Longman, London, UK, pp. 478.
- Didier, J., Dupraz, J., 1985. Magmatic and metasomatic cordierite in the Velay granite massif. In: Augusthitis, A. (Ed.), *The Crust: the Significance of Granite-Gneisses in the Lithosphere*. Theophrastus, Athens, GRE, pp. 35–77.

- Elphick, S.C., Ganguly, J., Loomis, T.P., 1985. Experimental determination of cation diffusivities in aluminosilicate garnets: i. Experimental methods and interdiffusion data. *Contrib. Miner. Petrol.* 90, 36–44.
- Franke, W., 1989. Tectonostratigraphic units in the Variscan belt of central Europe. *Geol. Soc. Am. Spec. Pap.* 230, 67–90.
- Franke, W., 2000. The mid-European segment of the Variscides: tectono-stratigraphic units, terrane boundaries and plate tectonic evolution. *Geol. Soc. Lond. Spec. Publ.* 179, 337–354.
- Frasl, G., Finger, F., 1991. Geologisch-petrographische Exkursion in den österreichischen Teil des südböhmisches Batholiths. *Beih. Eur. J. Mineral.* 3, 23–40.
- Fuchs, G., Matura, A., 1976. Zur Geologie des Kristallins der südlichen Böhmischen Masse. *Jb. Geol. B.-A.* 119, 1–43.
- Fuchs, G., Thiele, O., 1968. Erläuterungen zur Übersichtskarte des Kristallins im westlichen Mühlviertel und im Sauwald, Oberösterreich. *Geol. B.-A.*, Wien, Austria, 122 p.
- Groppi, C., Rolfo, F., Mosca, P., 2013. The cordierite-bearing anatectic rocks of the higher Himalayan crystallines (eastern Nepal): low-pressure anatexis, melt productivity, melt loss and the preservation of cordierite. *J. Metamorph. Geol.* 31, 187–204.
- Harker, A., 1939. Metamorphisms. A Study of the Transformations of Rock-Masses. Methuen, London UK, pp. 236.
- Hemingway, B.S., Robie, R.A., Apps, J.A., 1991. Revised values for the thermodynamic properties of boehmite, AlO(OH) , and comments on the relative stabilities of the aluminium hydroxide and the oxyhydroxide phases. *Am. Mineral.* 76, 445–457.
- Holdaway, M.J., Lee, S.M., 1977. Fe-Mg cordierite stability in high-Grade pelitic rocks based on experimental, theoretical, and natural observations. *Contrib. Mineral. Petrol.* 63, 175–198.
- Holdaway, M.J., 1971. Stability of andalusite and the aluminium silicate phase diagram. *Am. J. Sci.* 271, 97–131.
- Kalt, A., Altherr, R., Ludwig, T., 1998. Contact metamorphism in pelitic rocks on the island of Kos, Greece, Eastern Aegean Sea: a test for the Na-in-cordierite thermometer. *J. Petrol.* 39, 663–688.
- Kossmat, F., 1927. Gliederung des varistischen Gebirgsbaues. *Abh. Saechs. Geol. Landesanstalt* 1, 1–39.
- Leloup, P.H., Ricard, Y., Battaglia, J., Lacassin, R., 1999. Shear heating in continental strike-slip shear zones: model and field examples. *Geophys. J. Int.* 136, 19–40.
- Masch, L., Cetin, B., 1991. Gefüge, Deformationsmechanismen und Kinematik in ausgewählten Hochtemperatur-Mylonitzonen im Moldanubikum des Bayerischen Waldes. *Geol. Bavarica* 96, 7–27.
- Matte, P., 1986. Tectonics and plate tectonics model for the variscan belt of Europe. *Tectonophysics* 126, 329–374.
- Medaris, L.G., Jelínek, E., Míšar, Z., 1995. Czech eclogites: terrane settings and implications for Variscan tectonic evolution of the Bohemian Massif. *Eur. J. Mineral.* 7, 7–28.
- Medaris, L.G., Fournelle, J., Ghent, E.D., Míšar, Z., 1998. Prograde eclogite in the Gföhl Nappe, Czech Republic: new evidence on Variscan high-pressure metamorphism. *J. Metamorph. Geol.* 16, 563–576.
- Medaris, L.G., Wang, H.F., Jelínek, E., Mihaljevič, M., Jakeš, P., 2005. Characteristics and origins of diverse variscan peridotites in the gfohl nappe bohemian massif, Czech Republic. *Lithos* 82, 1–23.
- Medaris, L.G., Ghent, E.D., Wang, H.F., Jelínek, E., 2006. The spačiceclogite constraints on the P-T-t history of the gfohl granulite terrane, Moldanubian Zone, Bohemian Massif. *Mineral. Petrol.* 86, 203–220.
- Mirwald, P., 1986. Ist Cordierit ein Geothermometer? *Fortschr. Mineral.* 64/1, 113.
- O'Brien, P.J., Vrána, M., 1995. Eclogites with a shortlived granulite facies overprint in the Moldanubian Zone, Czech Republic: petrology, geochemistry and diffusion modelling of garnet zoning. *Geol. Rdsch.* 84, 473–488.
- O'Brien, P.J., 1997. Garnet zoning and reaction textures in overprinted eclogites, Bohemian Massif, European Variscides: a record of their thermal history during exhumation. *Lithos* 41, 119–133.
- Perchuk, L.L., Lavrent'eva, I.V., 1983. Experimental investigation of exchange equilibria in the system Cordierite-Garnet-Biotite. In: Saxena, S.K. (Ed.), *Kinetics and Equilibrium in Mineral Reactions*. Springer, New York, USA, pp. 199–239.
- Pereira, M.D., Bea, F., 1994. Cordierite-producing reactions in the Peña Negra complex, Avila Batholith, Central Spain: the key role of cordierite in low-pressure anatexis. *Can. Miner.* 32, 763–780.
- Petrakakis, K., 1986. Metamorphism of high-grade gneisses from the Moldanubian Zone, Austria, with particular reference to garnets. *J. Metamorph. Geol.* 4, 323–344.
- Petrakakis, K., 1997. Evolution of Moldanubian rocks in Austria: review and synthesis. *J. Metamorph. Geol.* 15, 203–222.
- Schreyer, H.P., Maresch, W.V., Daniels, P., Wolfsdorff, P., 1990. Potassic cordierites: characteristic minerals for high-temperature, very low pressure environments. *Contrib. Mineral. Petrol.* 105, 162–172.
- Schulmann, K., Kröner, A., Hegner, E., Wendt, L., Konopásek, J., Lexa, O., Štípká, P., 2005. Chronological constraints on the pre-orogenic history, burial and exhumation of deep-seated rocks along the eastern margin of the Variscan orogeny Bohemian Massif, Czech Republic. *Am. J. Sci.* 305, 407–448.
- Schulmann, K., Lexa, O., et al., 2008. Vertical extrusion and horizontal channel flow of orogenic lower crust: key exhumation mechanisms in large hot orogens? *J. Metamorph. Geol.* 26, 273–297.
- Seifert, F., 1976. Stability of the assemblage Cordierite + K-Feldspar + Quartz. *Contrib. Mineral. Petrol.* 57, 179–185.
- Selverstone, J., Morteani, G., Staude, J.M., 1991. Fluid channeling during ductile shearing: transformation of granodiorite into aluminous schist in the Tauern Window, Eastern Alps. *J. Metamorph. Geol.* 9, 419–431.
- Spear, F.S., 1991. On the interpretation of peak metamorphic temperatures in the light of garnet diffusion during cooling. *J. Metamorph. Geol.* 9, 379–388.
- Spear, F.S., 1993. Metamorphic Phase Equilibria and Pressure-Temperature-Time Paths. Mineral. Soc. Am., Washington D. C., USA, pp. 963.
- Steyrer, H.P., Sturm, R., 2002. Stability of zircon in a low-grade ultramylonite and its utility for chemical mass balancing: the shear zone at Miéville, Switzerland. *Chem. Geol.* 187, 1–19.
- Sturm, R., Steyrer, H.P., 2003. Use of accessory zircon for the quantification of volume changes in ductile shear zones cutting plutonic rocks. *Chem. Erde* 63, 31–54.
- Sturm, R., 1995. Geologisch-petrographische Bearbeitung eines cordieritführenden Mylonits und seiner Umrahmung im Bereich des Pfahls, oberösterreichisches Moldanubium Unpubl. Diploma Thesis. Univ. of Salzburg, Salzburg, Austria, pp. 169.
- Sturm, R., 2004. Volume balancing in ductile shear zones by the quantification of accessory zircon in oriented thin sections. *N. Jb. Min. Mh.* 180, 171–191.
- Sturm, R., 2010. Morphology and growth trends of accessory zircons from various granitoids of the South-western Bohemian Massif (Moldanubicum, Austria). *Chem. Erde* 70, 185–196.
- Wall, V.J., Clemens, J.D., Clarke, D.B., 1987. Models for granitoid evolution and source compositions. *J. Geol.* 95, 731–749.
- Wallbrecher, E., Brandmayr, M., Handler, R., Loizenbauer, J., Maderbacher, F., Platzer, R., 1993. Konjugierte Scherzonen in der südlichen Böhmischen Masse: Variszische und alpidische kinematische Entwicklungen (Projekt S4713). *Mitt. Österr. Min. Ges.* 138, 237–252.
- White, S.H., Burrows, S.E., Carreras, J., 1980. On mylonites in ductile shear zones. *J. Struc. Geol.* 2, 175–187.
- Yardley, B.W.D., 1990. An Introduction to Metamorphic Petrology. Longman, London, UK, pp. 326.
- Zoubek, V., 1965. Moldanubium und seine Stellung im geologischen Bau Europas. *Freiberger Forschungshefte* 190, 129–148.